Vol. 532: 13–28, 2015
doi: 10.3354/meps11336

MARINE ECOLOGY PROGRESS SERIES
Mar Ecol Prog Ser

Published July 21

Antarctic phytoplankton down-regulate their carbon-concentrating mechanisms under high CO_2 with no change in growth rates

Jodi N. Young[1,*], Sven A. Kranz[1,4], Johanna A. L. Goldman[1], Philippe D. Tortell[2,3], François M. M. Morel[1]

[1]Department of Geosciences, Princeton University, Princeton, NJ 08544, USA
[2]Department of Earth, Ocean and Atmospheric Sciences, University of British Columbia, Vancouver, BC V6T 1Z4, Canada
[3]Department of Botany, University of British Columbia, Vancouver, BC V6T 1Z4, Canada

[4]*Present address:* Department of Earth, Ocean and Atmospheric Sciences, Florida State University, Tallahassee, Fl 32306, USA

ABSTRACT: High-latitude oceans, in particular the coastal Western Antarctic Peninsula (WAP) region of the Southern Ocean, are experiencing a rapidly changing environment due to rising surface ocean temperatures and CO_2 concentrations. However, the direct effect of increasing CO_2 on polar ocean primary production is unclear, with a number of experiments showing conflicting results. It has been hypothesized that increased CO_2 may cause a reduction of the energy-intensive carbon concentrating mechanism (CCM) in phytoplankton, and these energy savings may lead to increased productivity. To test this hypothesis, we incubated natural phytoplankton communities in the WAP under high (800 ppm), current (400 ppm) and low (100 ppm) CO_2 for 2 to 3 wk during the austral spring-summer of 2012/2013. In 2 incubations with diatom-dominated phytoplankton assemblages, high CO_2 led to a clear down-regulation of CCM activity, as evidenced by an increase in half-saturation constants for CO_2, a decrease in external carbonic anhydrase activity and a higher biological fractionation of stable carbon isotopes. In a third incubation, there was no observable regulation of the CCM, possibly because HCO_3^- served as the major inorganic carbon source in all treatments for this phytoplankton assemblage. We did not observe a significant effect of CO_2 on growth rates or community composition in the diatom-dominated communities. The lack of a measureable effect on growth despite CCM down-regulation is likely explained by a very small energetic requirement to concentrate CO_2 and saturate Rubisco at low temperatures.

KEY WORDS: Phytoplankton · CO_2 · Antarctic · CCM · Growth

INTRODUCTION

Shelf waters surrounding Antarctica represent some of the most efficient sinks for anthropogenic CO_2 in the global ocean (Arrigo et al. 2008). The sink of CO_2 is largely driven by an extremely productive but highly seasonal phytoplankton community, which also provides the basis for the Antarctic marine food web (Ducklow et al. 2007). Rising anthropogenic CO_2 is partially absorbed by this sink (Le Quéré et al. 2007), and rapid changes in climate are being recorded, particularly in the Western Antarctic Peninsula (WAP) (Ducklow et al. 2013). For example, there has been a shift in the timing and magnitude of the phytoplankton bloom in the WAP, which has been attributed to shifting weather patterns and surface warming influencing water mixing (Montes-Hugo et al. 2009). Despite a growing understanding of the indirect, climate-related effects of CO_2 on marine ecosystems of the WAP, the direct effect of CO_2 on phytoplankton physiology remains poorly understood.

*Corresponding author: jny@princeton.edu

The low CO_2 buffering capacity of the polar oceans (Egleston et al. 2010) suggests these regions may be particularly sensitive to anthropogenic increases in CO_2. However, CO_2 concentrations in cold polar waters are already high relative to temperate regions due to the increased CO_2 solubility at cold temperatures (~25 µM at 0°C, air-equilibrated seawater). In addition, deep vertical mixing and upwelling of CO_2-rich deep water also leads to high CO_2 levels in polar waters, with early spring-time CO_2 concentrations along the WAP reaching ~30 µM, which is above the air-equilibrated value (Tortell et al. 2014). The high concentration of CO_2 in polar marine environments has led to the suggestion that photosynthesis is nearly CO_2-saturated via diffusion (Gleitz et al. 1996, Raven et al. 2002), though this has been contested (Riebesell et al. 1993). In addition, the enzyme responsible for carbon fixation, Ribulose 1,5 bisphosphate carboxylase oxygenase (Rubisco), has a lower half saturation constant for CO_2 (K_C) at cold temperatures (15 µM at 0°C compared to 45 µM at 20°C in diatoms; Young et al. 2015), and this difference reduces the concentration of CO_2 required for saturation at the site of fixation. Despite the high CO_2 concentrations in high-latitude waters and the increased substrate affinity of Rubisco in polar marine phytoplankton, many phytoplankton from polar environments do possess carbon-concentrating mechanisms (CCM). These CCMs act to elevate CO_2 concentrations at the site of Rubisco through the combined use of active bicarbonate transport, carbonic anhydrase activity (to catalyze CO_2 – HCO_3^- inter-conversion) and other components (for review, see Reinfelder 2011). Phytoplankton CCM activity has been clearly observed in polar marine waters (Cassar et al. 2004, Tortell et al. 2008b, 2010, Kranz et al. 2015) and in laboratory cultures of polar species (Mitchell & Beardall 1996, Trimborn et al. 2013). These CCMs are active at air-equilibrated seawater CO_2 concentrations and become increasingly important during phytoplankton blooms, when CO_2 concentrations can be reduced to as little as ~6 µM (Tortell et al. 2014).

The operation of a CCM is an energy intensive process, with different CCM strategies requiring various energy inputs (Raven et al. 2014). The CCM of many Antarctic phytoplankton measured in the field (Cassar et al. 2004, Tortell et al. 2008a) and in culture (Trimborn et al. 2013) involve ATP-dependent, active uptake of HCO_3^- across membranes, which use 0.5 ATP per HCO_3^- transported (Raven et al. 2014). It has been hypothesized that down-regulation of these energy intensive CCMs may liberate energy for growth (Giordano et al. 2005, Raven et al. 2011). In support of this hypothesis, incubation experiments have demonstrated increased primary production with increasing CO_2 in both the Antarctic (Tortell et al. 2008b, 2010, McMinn et al. 2014) and Arctic (Engel et al. 2012, Schulz et al. 2013).

It is unclear from laboratory experiments what is the mechanism whereby CCM down-regulation manifests as increased growth rates. Some studies have shown that acclimation at high CO_2 results in a decrease in photosynthetic machinery, including lower concentrations of chlorophyll *a* (chl *a*) (Sobrino et al. 2008) and Rubisco (Endo et al. 2015) per cell, while carbon fixation rates are maintained or increased, possibly due to enhanced photosynthetic efficiency at high CO_2 (Sobrino et al. 2008, Raven et al. 2011). In some cases, this increased photosynthetic efficiency only occurs under nutrient-limiting conditions, e.g. Fe limitation (Hopkinson et al. 2010). It has been shown in cyanobacteria that accumulation of carbohydrates under high CO_2 (i.e. high C:N) represses expression of photosynthetic genes (Woodger et al. 2005). However, other studies, including those of the Antarctic diatom *Chaetoceros brevis* showed little change in C:N, growth rates or the levels of chl *a* and Rubisco at high CO_2 (Boelen et al. 2011, Crawfurd et al. 2011). Furthermore, a study of 3 Antarctic diatoms and 1 Antarctic haptophyte species found CO_2-dependent regulation of CCM components (e.g. carbonic anhydrase activity) did not necessarily correspond with an effect on growth (Trimborn et al. 2013).

In this study, we report results from a series of CO_2 incubations conducted throughout the austral spring and summer of 2012/2013 in the coastal WAP. Our incubation experiments captured a range of phytoplankton assemblages over the course of a large seasonal CO_2 cycle. Incubations were initiated early in the season prior to the peak of phytoplankton biomass (I), during an intense diatom bloom (II), 1 mo after the bloom (III) and late in the season (IV). We examined the response of phytoplankton assemblages to varying CO_2 (from 100 to 800 ppm) in terms of growth, community composition and their physiology, including CCM activity.

MATERIALS AND METHODS

WAP sample collection and incubation setup

Incubations were conducted 4 times over the austral spring/summer 2012/2013 at the Palmer Long-Term Ecological Research (LTER) Station along the WAP. Seawater for incubations was collected from

LTER station B (64.7795° S, 64.0725° W) between late October 2012 and late March 2013 (Fig. 1). Water was pumped from a depth of 10 m into 20 l carboys using a monsoon pump (WSP-SS-80-NC, Waterra) deployed from a Zodiac. The collected water was stored under low light until returned to the station laboratories within ~1 h. Water was transferred to nine 4 l polycarbonate bottles and continuously bubbled in triplicate with the desired partial pressure of CO_2 (100, 400 and 800 ppm) in air delivered from commercially mixed standard tanks (Indura). Bottles were kept in on-deck incubators that were temperature controlled with circulating water drawn from 5 m depth and shaded using 1 layer of neutral density screening with 51.2% transmission (LEE filters). Surface irradiance (photosynthetically active radiation [PAR] between 400 and 700 nm) was obtained from meteorological sensors on the top of Palmer Station Laboratory. Over the course of the experiments, chl *a* and pH were measured daily and incubations were diluted twice during the 2 to 3 wk incubation with 0.2 µm filtered deep water (30 m) or surface water (10 m), to maintain exponential growth. The water used for dilution was collected at the same time as experimental water.

Measurements

Measurements of chl *a* and pH were taken daily. Other measurements were taken just prior to the 2 dilutions or/and at the end of the incubation. These time-points will be referred to 'early', 'middle' and 'end' as indicated in Fig. S1 in the Supplement at www.int-res.com/articles/suppl/m532p013_supp.pdf, along with the incubation length. The list of measurements collected at each time-point for each incubation is shown in Table S1 in the Supplement.

Carbonate chemistry and nutrients

Total alkalinity (TA) and pH were measured as described by Kranz et al. (2015). TA was measured in 0.2 µm filtered, mercury chloride-treated samples by potentiometric titration (Brewer et al. 1986). Seawater pH was determined by both potentiometry and spectrophotometrically using Thymol Blue (Zhang & Byrne 1996) with good correlation between the 2 methods (slope = 1.004, R^2 = 0.98, n = 81). The carbonate system was calculated from TA, pH, temperature, salinity, phosphate and silicate using CO2Sys. Equilibrium constants were those of Mehrbach et al. (1973) as refitted by Dickson & Millero (1987). Macro-nutrients (dissolved inorganic nitrogen (NO_3^- and NO_2^-), silicate and phosphate) were measured according to Joint Global Ocean Flux Study (JGOFS) protocols (Knap et al. 1996).

Chl *a* and pigment concentrations

Chl *a* and pigment concentrations were measured in accordance with Goldman et al. (2015). Chl *a* was extracted from samples filtered onto glass fiber filters (GF/F) following at least 12 h in 90% acetone and measured in un-acidified and acidified samples using a fluorometer (10-AU, Turner Designs) (Welschmeyer 1994). Growth rates were determined during the early, middle and late phase of the incubations from the logarithmic increase in chl *a* over 4 to 6 d. Pigments were extracted from GF/F filtered samples, flash frozen in liquid nitrogen and quantified using HPLC analysis performed by the Estuarine Ecology Lab (University of South Carolina) following the method of Pinckney et al. (1998). The abundance of pigments was measured as µg l^{-1}, and the relative abundance of accessory pigments were calculated as % contribution of total accessory pigments.

Particulate organic carbon (POC), nitrogen (PON) and $\delta^{13}C_{POC}$

POC, PON and $\delta^{13}C_{POC}$ were measured in the Princeton University isotope geochemistry lab following the method of Young et al. (2015). Samples for POC and PON were filtered onto pre-combusted 25 mm GF/F and acidified by fumigation with 6 N HCl overnight and dried at 60°C for 2 d. The whole filter was measured for POC, PON and $\delta^{13}C_{POC}$ using an elemental combustion analyzer (Costech) coupled to an isotope ratio mass spectrometer (DeltaV Advantage, Thermo Scientific). Measurements were calibrated against the standard reference material, peach leaf (NIST 2157) (Becker 1990), which was run in triplicate after every 8 samples. C:N ratios were calculated on a mole-mole basis from POC and PON on the filter.

$\delta^{13}C$ of dissolved inorganic carbon ($\delta^{13}C_{DIC}$) and the biological fractionation of stable carbon isotopes (εp)

Samples for $\delta^{13}C_{DIC}$ were collected from the incubation bottles with a peristaltic pump. Each sample

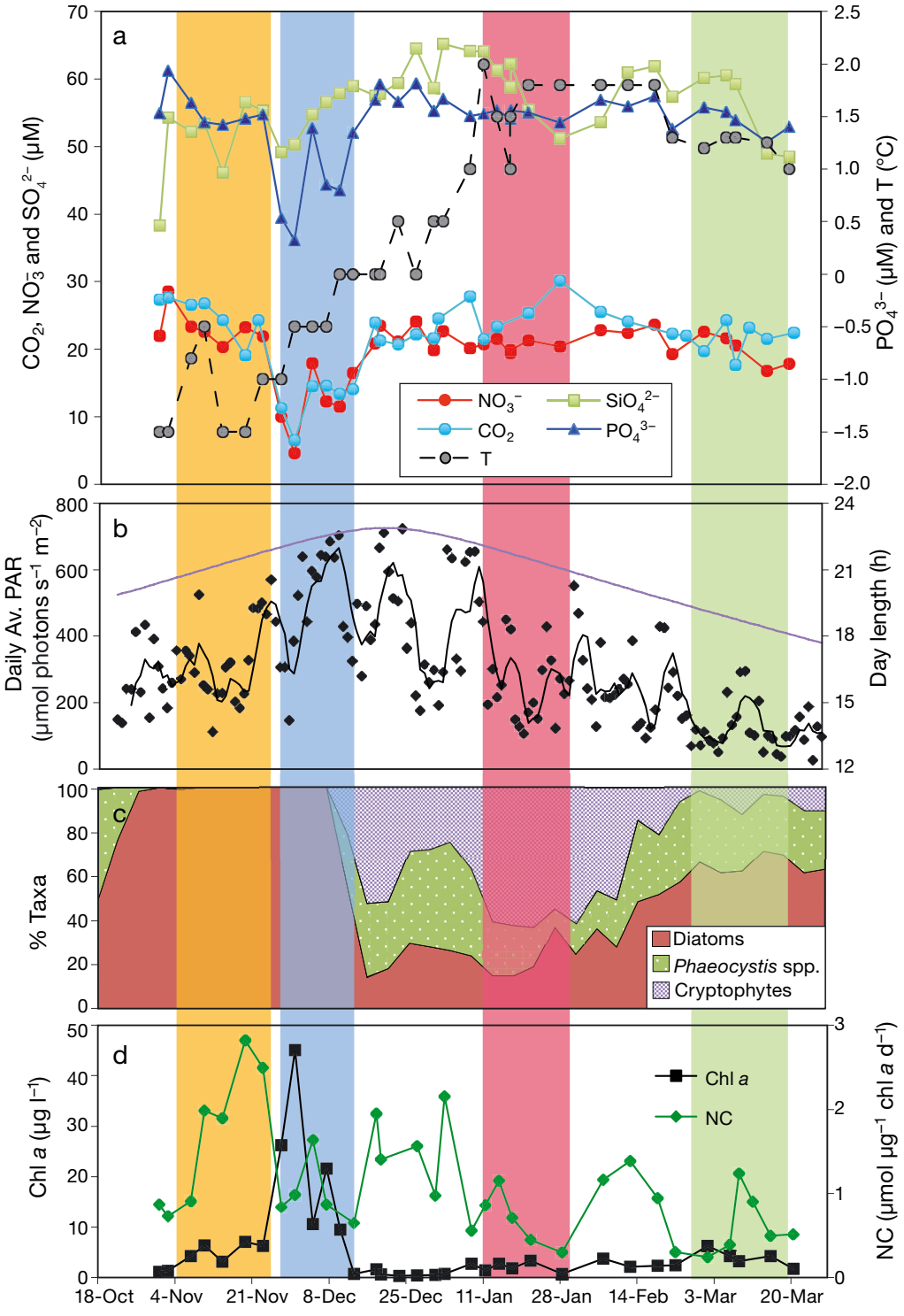

Fig. 1. Community and environmental conditions near shore at Palmer Station (Stn B), Western Antartic Peninsula (WAP), at 10 m depth during austral spring/summer 2012/2013. The timing of the 4 incubations I (orange), II (blue), III (red) and IV (green) are shown by vertical shading. (a) Concentrations of macronutrients: NO_3^- (red circles), SiO_4^{2-} (green squares) PO_4^{3-} (blue triangles) and CO_2 (aqua diamonds). Temperature (T) in °C shown by grey-filled black circles connected with a dashed line. (b) Light availability over the growing season. Daily average PAR (µmol photons s^{-1} m^{-2}) is shown by black diamonds with a 4 point running average (black line). Day length in hours is shown by purple line. (c) Percentage abundance of the dominant 3 classes of phytoplankton groups: diatoms (red), *Phaeocystis* spp. (green) and cryptophytes (purple). (d) Chlorophyll *a* concentrations (Chl *a*, µg l^{-1}, black squares) and chlorophyll normalized ^{14}C-based net carbon fixation rates (NC, µmoles C fixed µg^{-1} chl *a* d^{-1}, green diamonds)

was stored in a 16 ml borosilicate vial, spiked with 5 µl of saturated mercury chloride, capped with a Teflon coated rubber septum and stored at 2°C in the dark until analysis using a Carbon Isotope CRDS G2101-I (Picarro, Sunnyvale, CA). For the analysis, 10 ml of sample was transferred into a septum-sealed, N_2-sparged serum bottle (240 ml). Then, 30 µl of concentrated CO_2-free HCl was added to the sample to convert all DIC into CO_2. After a 30 min equilibration time, the CO_2 of the headspace was measured by flushing dried CO_2-free air (50 ml min^{-1}) through the bottle into the Carbon Isotope CRDS. The $\delta^{13}C$ signal intensity was measured after a steady state was reached (~5 min). The accuracy of the measurement, validated using a calcite standard (IAEA NBS18 calcite standard 5.014 ± 0.035‰ Vienna PeeDee Belemnite), averaged 4.9 ± 0.23‰ with a precision of ±0.31‰. $\delta^{13}C$ of CO_2 ($\delta^{13}C_{CO2}$) in the seawater samples was calculated from the isotopic mass balance as in Zhang et al. (1995) using $\delta^{13}C_{DIC}$, the concentrations of different inorganic carbon species and temperature-dependent equilibrium fractionation factors. Since the CO_2 in the mixed gas tanks had very low $\delta^{13}C$ (ca. −30‰) compared to the ambient CO_2 in seawater (ca. −10‰), the $\delta^{13}C_{CO2}$ within our incubations changed significantly over the course of the bubbling experiments. However, this did not have a large influence on εp as it only took ca. 1 d for the concentration of $CO_{2(aq)}$ in the bottles to match the tanks, whereas the biomass was sampled after at least 4 d of bubbling and the majority of the exponentially growing biomass is produced near the end of the incubation. εp was calculated from the $\delta^{13}C_{CO2}$ and $\delta^{13}C_{POC}$ using Eq. (1):

$$\varepsilon p = \frac{\delta^{13}C_{CO_2} - \delta^{13}C_{POC}}{1 + \frac{\delta^{13}C_{POC}}{1000}} \quad (1)$$

Primary production

Primary production estimates based on ^{14}C and ^{18}O incubations were carried out as in Goldman et al. (2015). ^{18}O incubation bottles (145 ml) were spiked with 125 µl $H_2{}^{18}O$ (Medical Isotopes, 97.6%), for a final enrichment of +412.4‰, and incubated for 4 to 9 h during maximum daylight under similar growth conditions. All samples were transferred into flasks that had been previously poisoned and evacuated. The flasks were analyzed for dO_2/Ar, $d^{18}O$ and $d^{15}N$ at Princeton University, within 6 mo, using a Delta Plus XP mass spectrometer (Thermo-Fisher Scientific) (Emerson et al. 1995). The change in O_2 concentration in the bottle during the incubation gives net photosynthesis in the light (NP_L), while the increase of [$^{18}O^{16}O$] provides gross photosynthesis (GP). Net carbon fixation (NC) was measured by spiking 125 ml of culture with 5 µCi $NaH^{14}CO_3$ and incubating for 24 h under similar growth conditions. ^{14}C-labelled organic carbon was measured in filtered and acidified samples using a liquid scintillation counter (LSC 6500, Beckman-Coulter).

Half-saturation constants for CO_2 (Km_{CO2})

Half-saturation constants for CO_2 (Km_{CO2}) of the community in the field were measured as performed by Tortell et al. (2010) and Kranz et al. (2015). Cells were concentrated by filtration on a 2 µm filter, resuspended in a CO_2-free buffer (pH 8.0; HEPES 50 µM), aliquoted into 1.5 ml tubes and spiked with varying concentrations of $NaH^{14}CO_3$. Carbon fixation during the 10 min incubation was determined by acidification of samples and measurement of ^{14}C-labelled organic carbon using a liquid scintillation counter (LSC 6500, Beckman-Coulter). The CO_2-dependent half-saturation constant for C fixation, Km_{CO2}, was calculated from least-squares estimates by fitting the data to a Michaelis-Menten hyperbolic equation. The standard error of the coefficient for Km_{CO2} was calculated for each curve fit. Only fits with p-values < 0.05 were included in the analysis.

Extracellular CA activity

Extracellular CA activity was measured according to Silverman (1982) by following ^{18}O exchange between CO_2 and HCO_3^- with a Quadrupole Mass Spectrometer (Pfeiffer Vacuum) connected to a temperature-controlled chamber via a gas permeable membrane (PTFE, 0.01 mm thick). The depletion of ^{18}O from aqueous $^{13}C^{18}O_2$ caused by the hydration and dehydration steps of CO_2 and HCO_3^- was measured in the dark in a concentrated culture that was resuspended in HEPES buffered seawater (pH 8.0, 2°C). A more detailed method description can be found in Kranz et al. (2015).

Rubisco content

Rubisco content relative to total protein was measured as performed by Losh et al. (2013) and Young et al. (2015). Total protein was extracted from GF/F fil-

tered cells in SDS buffer (50 mMTris-HCl, 2% SDS, 10% glycerol and 12.5 mM EDTA) and quantified using a BCA assay (Pierce, ThermoFisher Scientific). Rubisco content as a proportion of total protein was determined using quantitative western blots for the large subunit of Rubisco (RbcL) with global antibodies and standards (Agrisera) (Campbell et al. 2003). Concentrations of Rubisco protein were calculated from equimolar stoichiometry of the large and small (RbcS) subunit with molecular weights of 55 and 15 kDa, respectively (Baker et al. 1975). Note that our incubations contain a small presence of peridinin-containing dinoflagellates, which possess the form II Rubisco, which does not have a small subunit (Whitney et al. 1995), hence dinoflagellate Rubisco would be detected with our antibody but would produce error in our calculation by ~5% at the most.

Statistical analyses

Analysis of statistical significance ($p < 0.05$) among the 3 CO_2 treatments was conducted using 1-way ANOVA. Further analyses with ad-hoc tests (e.g. Tukey HSD) were not sensitive enough to detect significance due to the low sample size ($n < 3$) and the conservative nature of these tests.

RESULTS

The initial community and environment

Our incubations were initiated by sampling water from 10 m depth over the austral spring/summer to capture the range of community composition and environmental conditions during the growing season (Fig. 1; see also Tortell et al. 2014, Goldman et al. 2015, Kranz et al. 2015, Young et al. 2015). The first incubation (I) was initiated early in the season just after the sea ice had melted in late October. At the initiation of this incubation, water temperature was ca. −1°C, nutrients and CO_2 were high (e.g. NO_3^- was 23 µM and CO_2 was ~27 µM), and the community was composed principally of diatoms. The second incubation (II) was initiated at the beginning of an intense diatom bloom late November to early December, when nutrient and CO_2 drawdown was already apparent (10 µM drawdown for NO_3^- and 11 µM for CO_2) and water temperature was ca. −1 to 0°C. Incubation 3 (III) was initiated 1 mo after the bloom terminated in mid-January. The termination of the bloom was probably due to an increase in grazers, as well as a deep-water entrainment event (Tortell et al. 2014), which lead to a replenishment in surface macronutrients and CO_2 concentrations (21 µM NO_3^- and 20 µM CO_2). Following the bloom crash, phytoplankton biomass remained low and consisted of a mixed population of cryptophytes, diatoms and *Phaeocystis* spp.

We also conducted a fourth incubation (IV) late in the season (26 February to 19 March). The initial phytoplankton community was very similar to Incubation III but there was significantly lower light availability (for example, the day-length and daily maximum of PAR at the initiation of Incubations III and IV were 18 h and 12 h and 1800 and 650 µmol photons s^{-1} m^{-2}, respectively). The results of Incubation IV were very different to the other incubations and difficult to explain (e.g. very high $\delta^{13}C$ content of the biomass). For reasons that are not clear, we were also unable to get good replication for the CCM parameters. For these reasons, results from Incubation IV are not discussed within the main text. Rather, we present the results of this incubation experiment in the supplement and discuss potential factors (e.g. mixotrophy) that may have been at play.

Carbonate chemistry in the bottles

The pH measured in the various incubations was ~8.5, 8.0 and 7.8 at 100 ppm, 400 ppm and 800 ppm, respectively. Along with measured alkalinity, this resulted in $CO_{2(aq)}$ concentrations near the target values of 5 µM at 100 ppm, 25 µM at 400 ppm and 45 µM at 800 ppm (Fig. S2 and Table S2 in the Supplement). $CO_{2(aq)}$ concentrations varied somewhat around these target values as a result of changes in bubbling intensity and pCO_2 variability among the compressed gas cylinders (±20% of target value). The process of diluting the incubations with filtered water also led to short-lived perturbations in the carbonate system of the sampling bottles. During Incubation III, there was a drop in $CO_{2(aq)}$ just prior to the final sampling, which may have been due to insufficient bubbling rates. As expected, total dissolved inorganic carbon (DIC) changed little between treatments, only increasing ~1.2-fold between 100 and 800 ppm.

Community composition and pigments

The initial composition from the field was predominately diatom-dominated for the inoculation of Incubations I and II and a mixture of diatoms, cryptophytes and *Phaeocystis* spp. for the inoculation of

Incubation III (Fig. 1; Goldman et al. 2015). Phytoplankton below 2 µm in size were a negligible contribution to the communities. The community composition shifted over the course of the 2 to 3 wk incubations, as indicated by accessory pigments (Fig. 2). In all 3 incubations, CO_2 treatment had almost no effect on community composition, with the exception of Incubation II, in which peridinin, an indicator pigment for dinoflagellates, was present only at low CO_2. The large contribution of fucoxanthin in Incubations I and II suggest a diatom-dominated community, whereas Incubation III had an increased abundance of peridinin and 19′ hexanoyloxyfucoxanthin, along with fucoxanthin, suggesting a much more mixed community of diatoms, dinoflagellates and *Phaeocystis* spp. Alloxanthin, a diagnostic pigment for cryptophytes, was low in all incubations and suggests that the initial cryptophyte community in Incubation III did not take well to bottle incubations. There was also a high ratio of diatoxanthin:diadinoxanthin in Incubation I compared to Incubations II and III. Diatoxanthin is a photoprotective pigment and suggests the community may have been high-light stressed in Incubation I (Brunet et al. 1993). Microscopic analysis of the phytoplankton community at the end of Incubation II confirmed the dominance of diatoms and that there was no noticeable difference in composition or size between CO_2 treatments (see Fig. S3 in the Supplement at www.int-res.com/articles/suppl/m532p013_supp.pdf). Microscopic analysis was not done for Incubations I and III, thus a change in species composition or size with CO_2 cannot be completely discarded.

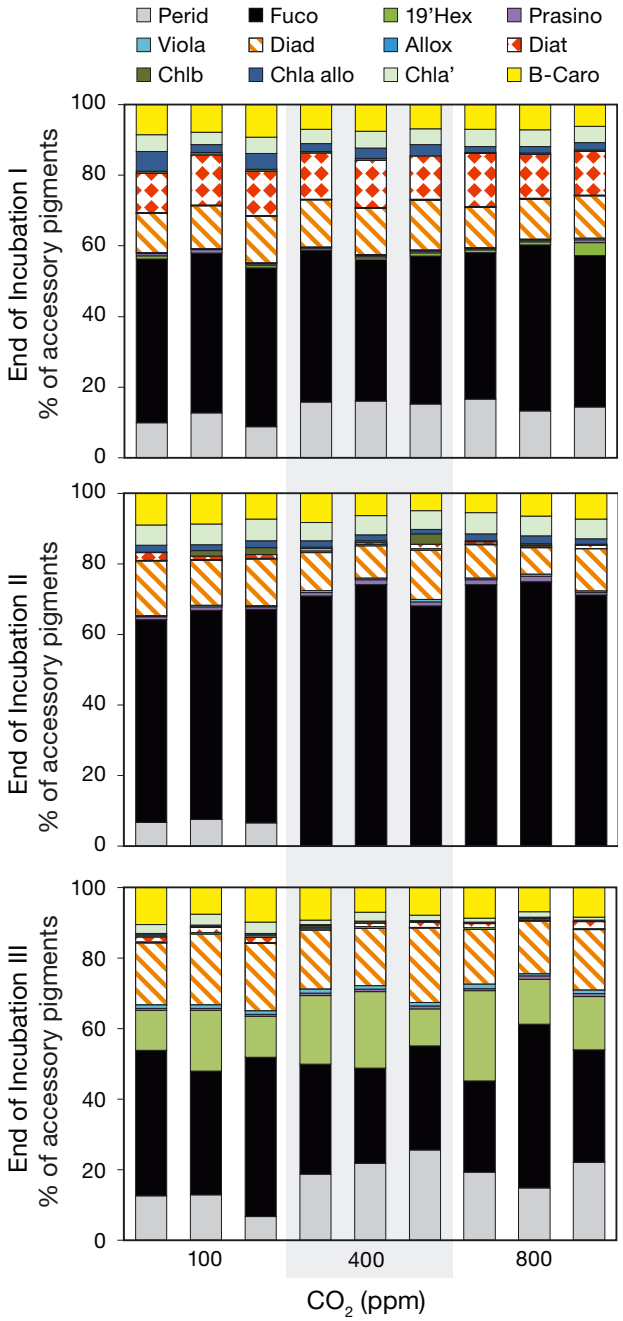

Fig. 2. Relative abundance of accessory pigments (as % w/w of contribution) in each bottle at the end of Incubations I to III: peridinin (Perid); fucoxanthin (Fuco); 19′hexanoyloxyfucoxanthin (19′Hex); prasinoxanthin (Prasino); violaxanthin (Viola); diadinoxanthin (Diad); alloxanthin (Allox); diatoxanthin (Diat); chlorophyll *b* (Chlb); chlorophyll *a* allomer (Chla allo); chlorophyll *a*′ (Chla′); β-carotene (B-Caro)

Cellular content and primary production rates

The concentrations of dissolved CO_2, dissolved N (NO_3^- + NO_2^-), particulate organic carbon (POC), particulate nitrogen (PN) and chl *a* are shown along with the subsequent ratios (POC:PN, POC:chl *a*, PN:chl *a*) in Table 1. CO_2 concentrations had little effect on POC:PN in all 3 incubations. At the time of harvest, dissolved nitrogen concentrations in Incubations I and II were very low and likely to be limiting. Dissolved N in Incubation III remained high and resulted in a higher PN:chl *a* compared to Incubations I and II. The availability of dissolved N seemed to exert a greater influence on POC:PN ratios of the biomass than CO_2, with Incubations I and II having ratios much higher (~7 to 8) than observed in Incubation III or in the field (~5; Young et al. 2015). Our results are similar to those of Losh et al. (2012) from the California current, who also found that N limitation had a much stronger influence than CO_2 on POC:PN in phytoplankton.

There was no trend of chl *a* concentrations with CO_2 throughout Incubations I and II (no shift in POC:chl *a*

Table 1. Concentrations of dissolved CO_2 (µM), dissolved inorganic nitrogen (NO_3^- + NO_2^-), particulate nitrogen (PN), chlorophyll *a* (Chl *a*), particulate organic carbon (POC) and subsequent ratios for each incubation (I, II, III) at each pCO_2 treatment. Samples were taken at the end of Incubations I and II, and early in Incubation III

	pCO_2 (ppm)	CO_2 (µM)	NO_3^- + NO_2^- (µM)	PN l^{-1} (µM)	Chl *a* l^{-1} (nM)	POC l^{-1} (µM)	POC:PN mol:mol	PN:chl *a* mol:mmol	POC:chl *a* mol:mmol
I	100	5.1 ± 0.1	0.3 ± 0.1	19.4 ± 1.4	25.7 ± 1.5	148 ± 7.9	7.6 ±0.2	0.76 ± 0.01	5.8 ± 0.1
	400	24.1 ± 0.7	0.3 ± 0.3	18.5 ± 0.9	23.3 ± 0.8	150.7 ± 8.1	8.2 ±0.2	0.79 ± 0.01	6.5 ± 0.2
	800	40.1 ± 1.0	0.2 ± 0.2	18.5 ± 1.2	26.9 ± 1.1	148.0 ± 10.0	8.0 ± 0.1	0.69 ± 0.06	5.5 ± 0.5
II	100	6.0 ± 1.0	0.0 ± 0.01	14.8 ± 0.4	26.2 ± 2.1	93.4 ± 4.9	6.3 ± 0.3	0.57 ± 0.04	3.6 ± 0.1
	400	27.0 ± 4.3	0.3 ± 0.3	16.6 ± 0.5	27.7 ± 2.1	100.7 ± 6.2	6.1 ± 0.1	0.6 ± 0.1	3.7 ± 0.5
	800	53.4 ± 2.5	1.8 ± 2.1	15.7 ± 2.9	25.4 ± 4.3	84.7 ± 28.3	5.3 ± 0.8	0.62 ± 0.04	3.3 ± 0.6
III	100	5.6 ± 0.1	17.1 ± 1.6	5.5 ±1.0	2.7 ± 0.8	29.1 ± 5.4	5.3 ± 0.1	2.08 ± 0.32	11.0 ± 1.6
	400	25.8 ± 0.8	15.3 ± 0.8	7.1 ± 0.2	4.8 ± 0.9	39.6 ± 1.9	5.6 ± 0.1	1.50 ± 0.24	8.4 ± 1.3
	800	47.1 ± 7.4	14.0 ± 2.9	8.0 ± 1.8	7.4 ± 4.1	44.2 ± 10.1	5.6 ± 0.1	1.21 ± 0.34	6.7 ± 1.9

or PN:chl *a*; Table 1, Fig. S4 in the Supplement). However, early in Incubation III, we observed an increase in chl *a* content with CO_2 (resulting in a lower ratio of both PN:chl *a* and POC:chl *a*). In Incubation III, there was a significant shift in community composition over the incubation, and it is likely that the early sampling represents a transitioning community. It is uncertain whether the trend of increased chl *a* content at high CO_2 persisted throughout Incubation III.

There was little influence of CO_2 on primary production based on rates of oxygen evolution and carbon fixation (Fig. 3). Rates of oxygen evolution in the light (4 to 9 h incubation), as determined by the change in O_2 concentration (net photosynthesis in the light [NP_L]) and the production of $^{18}O^{16}O$ (gross photosynthesis [GP]), were similar in all incubations and CO_2 treatments (~0.2 to 0.3 µmol O_2 $µg^{-1}$ chl *a* h^{-1}), and a very high ratio of NP_L:GP was found (~0.9 ± 0.15). These values are consistent with those found at Palmer Stn B during the diatom bloom (Goldman et al. 2015). In Incubation III only, there was slightly lower GP and NP_L under high (800 ppm) CO_2 as determined by 1-way ANOVA (GP: $F_{2,6}$ = 7.475, p = 0.041; NP_L: $F_{2,6}$ = 7.182, p = 0.02). Net primary production based on 24 h carbon fixation was also similar across all incubations and CO_2 treatments. However, there was a statistically significant difference in Incubation I ($F_{2,6}$ = 7.847, p = 0.021), where carbon fixation slightly increased at high CO_2 (800 ppm).

Growth rates

Despite the slight effects of high pCO_2 (800 ppm) on short-term primary production rates in some incubations, we did not observe any difference in phytoplankton growth rates. Growth rates, determined via exponential increases in chl *a* over 4 to 6 d, and the end of the incubations, after a ~2 wk acclimation to CO_2 treatment, were largely unaffected by CO_2 concentrations (Fig. 4a). In Incubations II and III, an increase in growth rates was observed over the course of the incubation (see Fig. S5 in the Supplement), probably indicating adaptation to bottle conditions. The maximum growth rates we observed in the incubation bottles (~0.5 d^{-1}) were similar to rates found in the spring diatom bloom at Stn B. We did observe a trend of increased growth rates with CO_2 early in Incubation III (Fig. S5c), but this is probably an artifact due to increasing chl *a* content per cell with CO_2. This trend was not maintained: by the middle and end of Incubation III, there was no correlation between CO_2 concentrations and chl *a*-derived growth rates.

CO_2 and the carbon concentrating mechanism (CCM)

While there was no influence of CO_2 on growth rates, we did observe a phytoplankton community response to CO_2 in terms of the regulation of their CCM. Measured parameters for CCM regulation included the half-saturation constant for CO_2 (Km_{CO2}), external carbonic anhydrase (eCA) activity and the biological fractionation of ^{13}C (εp).

Half-saturation constants for cellular carbon fixation (Km_{CO2}) were calculated from the generation of a Michaelis-Menten curve based on 10 min incubations of concentrated cells resuspended in buffered seawater pH 8.0 over a range of ^{14}C labeled DIC concentrations. In addition, the CO_2 saturation state of the cells (i.e. the rate presented as a percentage of the CO_2-saturated maximum rate) was derived from the Michaelis-Menten curve and the measured CO_2 concentration within each bottle. In Incubations I and

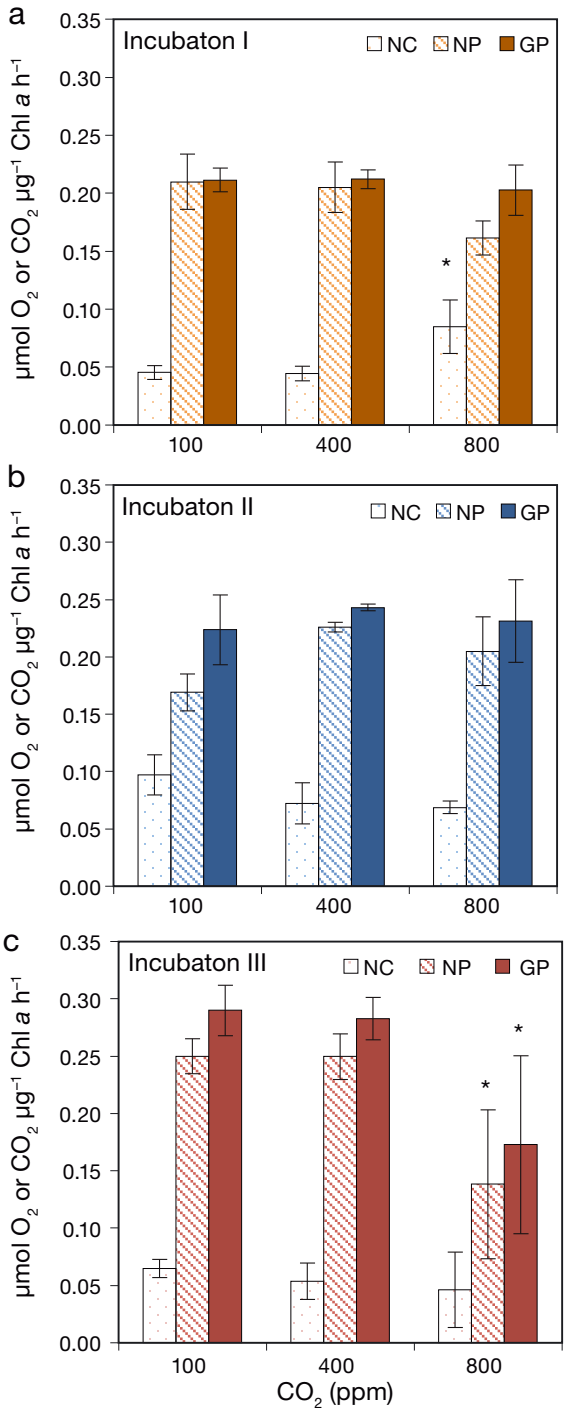

Fig. 3. Rates of short-term primary production. Net ^{14}C fixation (NC) over 24 h (open, dotted bar) at the end of Incubations (a) I, (b) II and (c) III. Net (NP, striped bar) and gross (GP, filled bar) oxygen production in the light (4 to 9 h), as determined through the change in O_2 concentration and production of $^{18}O^{16}O$, respectively. Due to sampling constraints, NP and GP for Incubation II were taken early in the incubation, whereas measurements from I and III were taken at the end. Error bars denote standard deviation from 3 biological replicates. *statistically significant difference ($p < 0.05$) using a 1-way ANOVA

II, which were dominated by diatoms, the Km_{CO2} was strongly positively correlated with pCO_2 (Fig. 4b; see Fig. S6 in the Supplement for curve fits to the ^{14}C data). In these experiments, cells maintained >80% saturation of C fixation across all pCO_2 treatments (Fig. 4c). This result is consistent with the measured saturation states of the natural community at Stn B during the field season (Kranz et al. 2015). In contrast with Incubations I and II, the Km_{CO2} calculated for phytoplankton assemblages during Incubation III did not vary systematically with pCO_2 treatments. The corresponding calculated CO_2 saturation state of the cells was <50% at the time of sampling in the low CO_2 treatment. This is highly unlikely since growth rates and carbon fixation rates are similar to the other incubations, and the data are most simply explained by considering that HCO_3^- was an important source of inorganic carbon for fixation by the cells in all treatments. Within the bottle incubations, HCO_3^- was abundant and varied little among CO_2 treatments. Calculating the degree of saturation of the cells using the DIC concentration in the bottle rather than CO_2 yields saturation >80% in all 3 cases (Table 2).

We also measured the activity of external carbonic anhydrase (eCA), an important component of the CCM that catalyzes the inter-conversion between HCO_3^- and CO_2 immediately outside the cell. eCA activity in Incubation I and II decreased markedly with increasing CO_2. In contrast, eCA activity in Incubation III exhibited no significant change across the pCO_2 treatments (Fig. 5a). The lack of CO_2-dependent eCA regulation in Incubation III mirrors what we observed with Km_{CO2}.

The biological fractionation of stable carbon isotopes (εp) also showed a positive correlation with CO_2, with an increase of up to 10‰ from 100 to 800 ppm (Fig. 5b; for raw data on δ^{13}_{CO2}, δ^{13}_{POC} and εp, see Table S3 in the Supplement). This result is consistent with field observations during the large spring diatom bloom where the strong drawdown of CO_2 resulted in low εp and low Km_{CO2} compared to those measured in the pre-bloom diatoms (Kranz et al. 2015). An increase in εp at high CO_2 can indicate a decrease in the proportion of HCO_3^- used as an inorganic carbon source, since HCO_3^- is ~10‰ heavier than CO_2 (Sharkey & Berry 1985). Alternatively, it can indicate replenishment of isotopic equilibrium of the intracellular carbon pool, which can be achieved via higher external CO_2 concentrations or increased gross CO_2 fluxes across membranes (Keller & Morel 1999, Hopkinson et al. 2011).

We found no correlation between Rubisco content and CO_2 in any of the incubations. However, we ob-

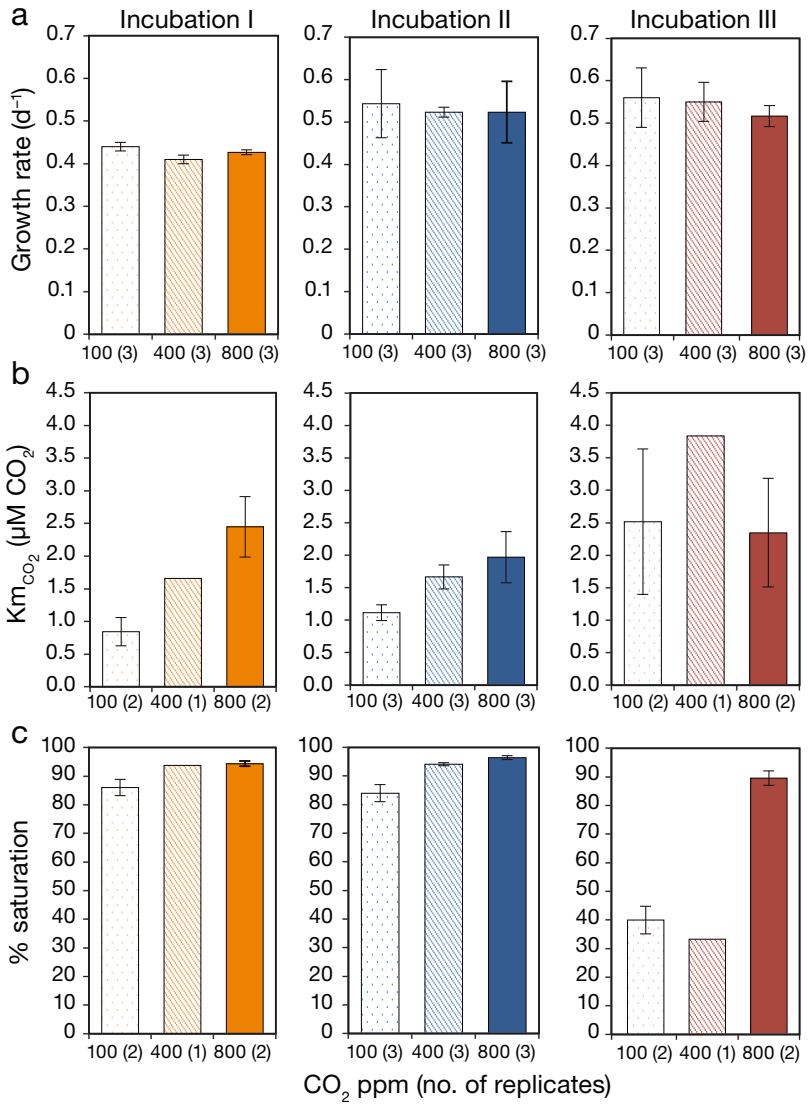

Fig. 4. The effect of treatments of low (100 ppm, open dotted bar), ambient (400 ppm, striped bar) and high (800 ppm, filled bar) CO_2 measured at the end of Incubations I, II and III on (a) growth rates (d^{-1}) based on the exponential increase of chlorophyll *a* (µg l^{-1}) over ~5 d, (b) the half saturation constant for CO_2 (Km_{CO2}), which is the CO_2 concentration (µM) that results in half the maximum rate, and (c) the percentage (%) that the cells are saturated by CO_2. Numbers in brackets show number of biological replicates, and error bars denote standard deviation of the replicates. See the Supplement at www.int-res.com/articles/suppl/m532p013_supp.pdf for raw data and curve fits

Table 2. Percentage saturation (±1 SD) of carbon fixation at each pCO_2 treatment calculated using either CO_2 or total dissolved inorganic carbon (DIC) as a substrate. n: number of replicates

pCO_2 treatment	I			II			III		
	CO_2	DIC	n	CO_2	DIC	n	CO_2	DIC	n
100	86 ± 2	95 ± 0.1	2	84 ± 3	94 ± 0.6	3	40 ± 5	85 ± 5	2
400	94 ± nd	92 ± nd	1	94 ± 0.6	92 ± 0.7	3	33	80 ± 6	1
800	94 ± 0.9	89 ± 1.8	2	96 ± 0.7	91 ± 1.6	3	89 ± 2.5	89 ± 3	2

served a positive correlation between Rubisco content (as a percentage of total protein) and growth rate (Fig. 6). The increase in Rubisco content and growth rate from early to the end of Incubation III likely represents adaptation of the phytoplankton communities in the bottle. By the end of Incubation II (blue circles) and III (red triangles), growth rates and Rubisco abundance (as a percentage of total protein) were similar to those found in the field during the diatom bloom (Young et al. 2015).

DISCUSSION

Our incubation experiments with natural phytoplankton assemblages from the Western Antarctic Peninsula at different pCO_2 levels revealed 2 main responses in our diatom dominated incubations: (1) varying pCO_2 had no measurable effect of the growth rates; (2) there was a clear and strong down-regulation of the CCM with increasing pCO_2.

This study measured the effect of CO_2 on 3 distinct phytoplankton communities. Incubations I and II were diatom-dominated, whereas Incubation III was a more mixed community of diatoms, dinoflagellates and *Phaeocystis* spp. The high ratio of diatoxanthin to diadinoxanthin in Incubation I suggests the community is adapted to high light as diatoxanthin is produced by diatoms, dinoflagellates and haptophytes as a photoprotective pigment (Brunet et al. 1993, Schumann et al. 2007). The community in the bottles at the end of the incubation had shifted from the initial field community inoculated at the beginning, probably due to 'bottle-effects', which can influence community composition (Venrick et al. 1977), size (Hammes et al. 2010) and primary production rates (Fogg & Calvario-Martinez 1989). Bottle effects are caused by the

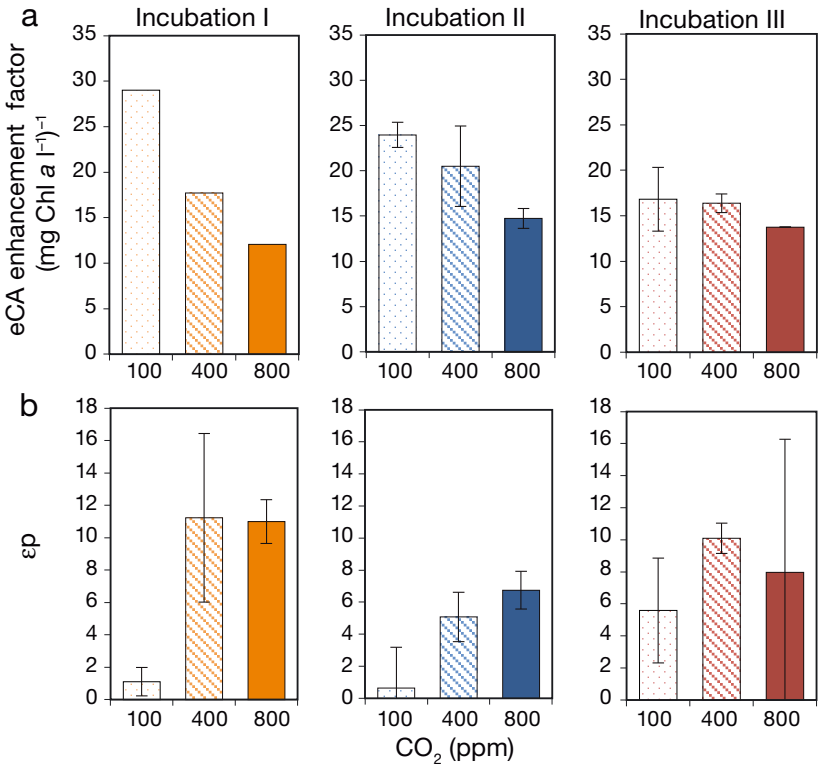

Fig. 5. (a) External carbonic anhydrase (eCA) enhancement factor, as measured by following ^{18}O exchange between CO_2 and HCO_3^- and expressed as relative enhancement of the uncatalyzed rate. Incubation I was measured from pooled triplicate samples, whereas Incubations II and III show standard deviation of biological triplicates, all measured at the end of the incubations. (b) The biological fractionation of stable carbon isotopes (εp) measured at the end of the incubation for I and II and early in Incubation III. Error bars denote standard deviation of 3 biological replicates. $\delta^{13}C_{CO2}$ and $\delta^{13}C_{POC}$ used to derive εp are shown in Table S3 in the Supplement

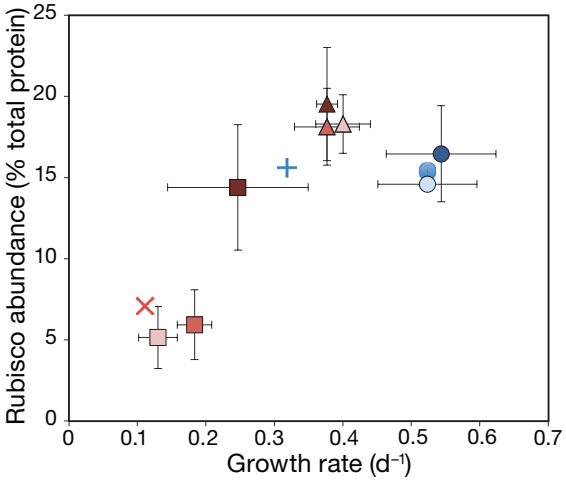

Fig. 6. Rubisco abundance as percentage of total protein plotted against growth rates (d^{-1}). For Incubation II (blue), values were taken at the initiation (+) and at the end (circles). For Incubation III (red), values were taken at the initiation (×), early (squares) and at the end (triangles). Increasing color intensity from light to dark indicates increasing CO_2 concentrations. The error bars are standard deviations of 3 biological replicates

artificial environment created by the enclosure of the natural phytoplankton community within a bottle, which removes mixing, prevents the exchange of nutrients with the surrounding waters and excludes large grazers (Calvo-Díaz et al. 2011).

Despite the difference in community composition and physiology between incubations, the rates of growth and primary production were remarkably similar. Growth rates in all incubations were similar to those found during the diatom bloom sampled at Stn B (~0.5 d^{-1}). Similar growth rates (as determined through cell counts) of psychrophilic algae have been observed in the laboratory and the field (Gilstad & Sakshaug 1990, Timmermans et al. 2001), one exception being the high growth rates of the diatoms *Chaetoceros debilis* and *Pseudo-nitzschia subcuvata* in laboratory experiments of Trimborn et al. (2013). In this study, growth rates were normalized to chl *a*, and some studies have observed a decrease in chl *a* with increasing CO_2 (e.g. Sobrino et al. 2008), which would produce errors in our growth rate estimates. However, we found no effect of CO_2 on chl *a* throughout our diatom-dominated Incubations I and II, though there was an increase in chl *a* with CO_2 early in Incubation III, which artificially increased growth rates at high CO_2. While we have no measurements of chl *a*:POC later in Incubation III, chl *a* normalized growth rates show no CO_2 effect by the middle or at the end of the incubation. It is likely that once the cells (and thus the chl *a* content) have acclimated to the different CO_2 concentrations, the rate of increase in chl *a* concentrations over time will be indicative of growth rate and not of changing cellular content.

In general, growth rates increased over the course of the incubations, and this is likely the result of the adaptation of the community to the conditions in the bottles. Interestingly, the increase in growth rates over the course of the incubation was paralleled by an increase in the concentration of Rubisco (Fig. 6). This result is in agreement with the idea that the carboxylation by Rubisco may be the limiting step in photosynthesis in cold-water phytoplankton (Young et al. 2015).

In Incubation I, we observed an increase in net carbon fixation (NC, measured by ^{14}C over 24 h normalized to chl *a*) at high pCO_2, whereas in Incubation III, we observed a decrease in oxygen evolution (both NP_L and GP in the light). These opposite responses are likely explained by the different parameters that are measured by the 2 techniques. In particular, a decrease in dark respiration at high pCO_2 (and low pH), as observed in a previous field study (Hopkinson et al. 2010), would increase net carbon fixation measured by ^{14}C without affecting the evolution of O_2 in the light. Other explanations include variation in the production of dissolved organic carbon, which would not be accounted for in ^{14}C fixation.

It is well known that many Antarctic phytoplankton utilize carbon concentrating mechanisms (CCMs) (Tortell et al. 2008b, 2010, 2013, Trimborn et al. 2013, Kranz et al. 2015), and it has been suggested that down-regulation of the CCM in response to high CO_2 may free up energy for growth (Giordano et al. 2005, Raven et al. 2011). While we did not observe a CO_2 influence on growth, we did observe clear down-regulation of the CCM with increasing pCO_2 in the 2 diatom-dominated incubations. Down-regulation of the CCM was shown through increased CO_2 half-saturation constants for cellular carbon fixation (Km_{CO2}), decreased external carbonic anhydrase activity (eCA) and increased biological fractionation of stable carbon isotopes (εp).

The lack of CO_2-dependent CCM regulation in Incubation III is interesting. This is consistent with observations that the photosynthetic apparatus is saturated only if one considers total dissolved inorganic carbon (DIC) as a substrate instead of CO_2. One possible explanation is that the dominant species in the Incubation III (mix of *Phaeocystis* spp. diatoms and dinoflagellates) may chiefly take up bicarbonate. The use of bicarbonate as the predominant source of carbon has been observed in *Phaeocystis*-dominated Ross Sea phytoplankton assemblages (Tortell et al. 2010) and at the height of the diatom bloom in the WAP in the same season as our incubations (Kranz et al. 2015). In Incubation III, the dominant use of bicarbonate may be due to the sudden shift in $CO_{2(aq)}$ concentrations just prior to sampling. We note that this drop in CO_2 resulted in narrowed range of pCO_2 concentrations between treatments.

The CO_2 half-saturation constant for cellular carbon fixation (Km_{CO2}) in all 3 incubations was considerably lower than the concentration of ambient $CO_{2(aq)}$ in the incubation bottles and lower than the CO_2 half-saturation constant of Rubisco (K_C). This provides direct evidence for an operational CCM under all pCO_2 treatments. Remarkably, the Km_{CO2} increased with increasing CO_2 in such a way that the cells maintained CO_2 saturation just over 80%. This result suggests a tight regulation of carbon uptake kinetics with external CO_2 concentrations. Components of the CCM that may be regulated to maintain 80% saturation include increasing carbonic anhydrase activity (as shown in Fig. 5a) and bicarbonate transport (as shown during an Antarctic diatom bloom by Kranz et al. 2015).

Our results agree with those of Kranz et al. (2015), who found that phytoplankton were able to regulate Km_{CO2} to maintain nearly 80% during the diatom bloom in the WAP despite a large drawdown of CO_2. A positive correlation between Km_{CO2} and CO_2 concentrations has been observed previously in Amundsen phytoplankton assemblages (Tortell et al. 2013) and in *Phaeocystis*-dominated Ross Sea phytoplankton communities (Tortell et al. 2010), albeit over a much wider range in Km_{CO2}.

The role of external carbonic anhydrase (eCA) in the CCM is to maintain a high CO_2 concentration at the cell surface (Elzenga et al. 2000), which may be particularly important during the bloom when external CO_2 concentrations are low and diffusion is slow. The down-regulation of eCA activity in Incubations I and II agrees with the laboratory study of Trimborn et al. (2013), who found decreased eCA activity in all the Antarctic phytoplankton under high CO_2 conditions. In contrast, Tortell et al. (2010, 2013) and Kranz et al. (2015) found no significant correlation of eCA activity and pCO_2 in the field (WAP and Ross Sea) or in cultures of *Fragilariopsis cylindrus*. These differences may reflect the small energy benefit provided by eCA (Hopkinson et al. 2013, Kranz et al. 2015), which may be essential only when CO_2 levels are very low (<1 µM) (Burkhardt et al. 2001). In Incubation III, which we suggest relies on HCO_3^- as the dominant source of inorganic carbon, eCA activity is still present. However, eCA activity is lower in Incubation III compared to the other incubations at low CO_2, further supporting a HCO_3^- dominant uptake mechanism. Nonetheless, CO_2 may still be taken up to some extent in Incubation III, requiring the need of some eCA to elevate CO_2 concentrations around the cell while having little effect on the HCO_3^- concentration.

We observed a positive correlation between the biological fractionation of stable carbon isotopes (εp) and CO_2, which was also seen during a large diatom bloom in the WAP (Kranz et al. 2015). A recent field study in the Amundsen Sea (Tortell et al. 2013) found a similar negative correlation between $\delta^{13}C_{POC}$ and

growth rates/pCO_2. As growth rates were similar across our different CO_2 incubation treatments, the variation in $\delta^{13}C$ must be primarily dependent on ambient CO_2 concentrations. A compilation of field and laboratory studies over a range of temperatures (Tortell et al. 2000) observed that the non-linear decrease of εp with increasing growth rates/CO_2 could only be explained with active uptake of inorganic carbon (i.e. a CCM) (Tortell et al. 2000). A model of an Antarctic diatom CCM based on field data (Kranz et al. 2015) demonstrated that εp is largely driven by the gross fluxes of inorganic carbon in and out of the cell due to the high membrane permeability of CO_2. As external CO_2 concentrations decrease, these gross fluxes also decrease, leading to a higher intracellular ^{13}C concentration. These gross fluxes dominate the signal of $\delta^{13}C_{POC}$ and explain why a shift in the proportion of HCO_3^- uptake has little influence on $\delta^{13}C_{POC.}$

While a number of mechanisms can explain an increase of εp at high CO_2, the results of modeling the Antarctic spring diatom bloom (Kranz et al. 2015), suggest that an increase in εp is more likely due to a larger exchange of intracellular DIC via CO_2 diffusion across membranes than a decrease in relative HCO_3^- utilization.

Our finding that pCO_2 had little effect on phytoplankton growth rates agrees with the results of Trimborn et al. (2013) for the majority of Antarctic phytoplankton tested (2 of 3 different genera of Antarctic diatoms and a *Phaeocystis* sp.). Nonetheless, Trimborn et al. (2013) observed that the fast-growing diatom species *Chaetoceros debilis* (see above) increased its growth rate in response to rising CO_2. This appears to be a species-specific response, as another species from the same genus, *Chaetoceros brevis,* showed no CO_2 response in growth or composition (Boelen et al. 2011). Field studies have demonstrated variable effects of CO_2 on the growth of Antarctic phytoplankton. In incubations of natural Ross Sea phytoplankton assemblages (mixed diatoms and *Phaeocystis* spp.), growth and net carbon fixation rates increased by around 10 to 20% with high CO_2 as the communities transitioned from pennate diatoms to larger centric diatom species (*Chaetoceros* spp.; Tortell et al. 2008b). However, in another Ross Sea study, high pCO_2 had no effect on net (24 h) carbon fixation but decreased both short-term carbon fixation rates and CCM activity in a *Phaeocystis* spp.-dominated community (Tortell et al. 2010).

Some laboratory studies have shown that acclimation to high CO_2 results in the down-regulation of the entire photosynthetic machinery in phytoplankton due to enhanced energy efficiency of photosynthesis through down-regulation of the CCM (Sobrino et al. 2008). In our diatom-dominated communities, we observed no down-regulation of photosynthetic machinery (chl *a* or Rubisco) with CO_2, despite clear down-regulation of their CCM. Our findings are also consistent with the suggestion that photosynthetic gene expression is repressed by carbohydrate accumulation (Woodger et al. 2005), as we also observed that CO_2 had little effect on POC:PN ratios. We hypothesize that the low energy savings produced from CCM down-regulation at cold temperatures (see below), along with the high protein levels required to maintain photosynthesis (e.g. Rubisco; Young et al. 2015) imply that psychrophilic diatoms are unlikely to be able to increase photosynthetic efficiency at high CO_2.

The apparent paradox of CCM down-regulation without significant changes in growth rates may be explained by the relatively low energy requirements of the CCM in cold-water phytoplankton. This low energetic requirement stems principally from 2 factors: (1) the high solubility of CO_2 in seawater at cold temperatures; (2) the low CO_2 half-saturation constant of Rubisco (K_C) at low temperature (Young et al. 2015). For example, the solubility of CO_2 is ~25 µM in air-equilibrated seawater at 0°C, while the K_C for diatom Rubisco is ~15 µM. These values change to 13 and 45 µM, respectively at 20°C (Young et al. 2015).

The bulk of the energy required for the CCM comes from the active transport of bicarbonate into the chloroplast to make up for the passive loss of CO_2 by diffusion. The net result is that this energy requirement is roughly proportional to the gradient of CO_2 from the site of fixation to the bulk seawater. To calculate the energetic cost of the CCM, we followed the calculation by Kranz et al. (2015) for a diatom cell of 20 µm in diameter and a concentration of 60 µM CO_2 in the pyrenoid (to obtain 80% saturation of Rubisco with a K_C of 15 µM). We found the energetic cost of the CCM to be 157, 100 and 28 kJ for each mole of CO_2 fixed at 100, 400 and 800 ppm, respectively (Table 3). Thus, between 100 and 800 ppm, there is an energy saving of 129 kJ. This is a relatively small fraction of the 2438 to 2840 kJ required to fix 1 mole CO_2 into biomass (Buchanan et al. 2000, Boyle & Morgan 2011) (590 kJ is required just for the Calvin Cycle, 3ATP + 2 NADPH; Falkowski & Raven 2007). Furthermore, it is likely that cold-water phytoplankton are not energy limited, as alternative processes that generate ATP, e.g. cyclic electron flow around PSI, have been shown to be highly active (Goldman et al. 2015).

Table 3. Calculated flux of CO_2 from a 20 µm diameter polar diatom at various CO_2 treatments. Pyrenoid [CO_2] was set as the concentration required to achieve 80% CO_2 saturation of Rubisco with a Kc of 15 µM. Flux was calculated as the CO_2 gradient between external and pyrenoid, multiplied by the mass transfer coefficient for the pyrenoid (4.5×10^{-9} cm^3 s^{-1}) for a diatom cell with a 20 µm diameter (Kranz et al. 2015). A negative value indicates a flux out of the cell. Energy loss was calculated from the estimation of 4 moles CO_2 leaked for every 1 mole of CO_2 fixed at 400 ppm (Kranz et al. 2015) and assuming active transport of bicarbonate is through a SLC4 type bicarbonate transporter with an energetic cost of 0.5 ATP per bicarbonate transported (Hopkinson et al. 2011, Nakajima et al. 2013)

CO_2 treatment (ppm)	External [CO_2] (µM)	Pyrenoid [CO_2] (µM)	Flux (fmoles CO_2 s^{-1} $cell^{-1}$)	Fold leakage normalised to 400 ppm	Energy loss (kJ per mole of CO_2)
100	5	60	−0.25	1.57	157
400	25	60	−0.16	1.00	100
800	50	60	−0.05	0.29	28

CONCLUSIONS

Phytoplankton in the coastal Western Antarctic Peninsula provide the basis for an extremely productive food web and are responsible for a large biological sink of CO_2 from the atmosphere. While this region is particularly sensitive to climate change, the direct effects of increasing CO_2 on phytoplankton community, production and cellular composition appear small. This is despite the fact that some phytoplankton clearly respond to increasing CO_2 by down-regulating their carbon concentrating mechanism. However, the energy savings of this down-regulation does not appear to be sufficient for an observable increase in growth rate and primary production, and thus the direct effect of rising CO_2 on phytoplankton productivity in this region may be limited.

Acknowledgements. We acknowledge the exceptional assistance provided by the science support and administrative staff at Palmer Station and the entire Palmer LTER science team. We thank Jay Pinckney for running the HPLC samples and Brian Hopkinson for advice on calculating CCM energy savings. This study was funded by the US National Science Foundation (OPP 1043593, EF 1040965, OCE 0825192). Funding to PDT was provided by the Natural Science and Engineering Research Council of Canada. We acknowledge the anonymous reviewers for their insightful comments

LITERATURE CITED

Arrigo KR, van Dijken G, Long M (2008) Coastal Southern Ocean: A strong anthropogenic CO_2 sink. Geophys Res Lett 35:L21602, doi:10.1029/2008GL035624

Baker TS, Eisenberg D, Eiserling FA, Weissman L (1975) The structure of form I crystals of D-ribulose-1,5-diphosphate carboxylase. J Mol Biol 91:391–398

Becker DA (1990) Homogeneity and evaluation of the New NIST Leaf Certified Reference Materials. Biol Trace Elem Res 26–27:571–577

Boelen P, van de Poll WH, van der Strate HJ, Neven IA, Beardall J, Buma AGJ (2011) Neither elevated nor reduced CO_2 affects the photophysiological performance of the marine Antarctic diatom *Chaetoceros brevis*. J Exp Mar Biol Ecol 406:38–45

Boyle NR, Morgan JA (2011) Computation of metabolic fluxes and efficiencies for biological carbon dioxide fixation. Metab Eng 13:150–158

Brewer PG, Bradshaw AL, Williams RT (1986) Measurements of total carbon dioxide and alkalinity in the North Atlantic Ocean. In: Trabalka JR, Reichle DE (eds) The changing carbon cycle: a global analysis. Springer, New York, NY, p 348–370

Brunet C, Brylinski JM, Lemoine Y (1993) *In situ* variations of the xanthophylls diatoxanthin and diadinoxanthin: photoadaptation and relationships with a hydrodynamical system in the eastern English Channel. Mar Ecol Prog Ser 102:69–77

Buchanan BB, Gruissem W, Jones RL (eds) (2000) Biochemistry and molecular biology of plants. American Society of Plant Physiologists, Rockville, MD

Burkhardt S, Amoroso G, Riebesell U, Sültemeyer D (2001) CO_2 and HCO_3^- uptake in marine diatoms acclimated to different CO_2 concentrations. Limnol Oceanogr 46: 1378–1391

Calvo-Díaz A, Díaz-Pérez L, Suárez LÁ, Morán XAG, Teira E, Marañón E (2011) Decrease in the autotrophic-to-heterotrophic biomass ratio of picoplankton in oligotrophic marine waters due to bottle enclosure. Appl Environ Microbiol 77:5739–5746

Campbell DA, Cockshutt AM, Porankiewicz-Asplund J (2003) Analysing photosynthetic complexes in uncharacterized species or mixed microalgal communities using global antibodies. Physiol Plant 119:322–327

Cassar N, Laws EA, Bidigare RR, Popp BN (2004) Bicarbonate uptake by Southern Ocean phytoplankton. Global Biogeochem Cycles 18:GB2003, doi:10.1029/2003GB002116

Crawfurd KJ, Raven JA, Wheeler GL, Baxter EJ, Joint I (2011) The response of *Thalassiosira pseudonana* to long-term exposure to increased CO_2 and decreased pH. PLoS ONE 6:e26695

Dickson AG, Millero FJ (1987) A comparison of the equilibrium constants for the dissociation of carbonic acid in seawater media. Deep-Sea Res 34:1733–1743

Ducklow HW, Baker K, Martinson DG, Quetin LB and others (2007) Marine pelagic ecosystems: the West Antarctic Peninsula. Philos Trans R Soc Lond B 362:67–94

Ducklow HW, Fraser W, Meredith MP, Stammerjohn SE and others (2013) West Antarctic Peninsula: an ice-depen-

dent coastal marine ecosystem in transition. Oceanography (Wash DC) 26:190–203

Egleston ES, Sabine CL, Morel FMM (2010) Revelle revisited: buffer factors that quantify the response of ocean chemistry to changes in DIC and alkalinity. Global Biogeochem Cycles 24, GB1002, doi:10.1029/2008GB003407

Elzenga JTM, Prins HBA, Stefels J (2000) The role of extracellular carbonic anhydrase activity in inorganic carbon utilization of *Phaeocystis globosa* (Prymnesiophyceae): a comparison with other marine algae using the isotopic disequilibrium technique. Limnol Oceanogr 45:372–380

Emerson S, Quay PD, Stump C, Wilbur D, Schudlich R (1995) Chemical tracers of productivity and respiration in the subtropical Pacific Ocean. J Geophys Res C 100: 15873–15887

Endo H, Sugie K, Yoshimura T, Suzuki K (2015) Effects of CO_2 and iron availability on *rbcL* gene expression in Bering Sea diatoms. Biogeosciences 12:2247–2259

Engel A, Borchard C, Piontek J, Schulz K, Riebesell U, Bellerby R (2012) CO_2 increases ^{14}C-primary production in an Arctic plankton community. Biogeosciences Discuss 9:10285–10330

Falkowski PG, Raven JA (2007) Aquatic photosynthesis, Vol 2. Princeton University Press, Princeton, NJ

Fogg GE, Calvario-Martinez O (1989) Effects of bottle size in determinations of primary productivity by phytoplankton. Hydrobiologia 173:89–94

Gilstad M, Sakshaug E (1990) Growth rates of ten diatom species from the Barents Sea at different irradiances and day lengths. Mar Ecol Prog Ser 64:169–173

Giordano M, Beardall J, Raven JA (2005) CO_2 concentrating mechanisms in algae: mechanisms, environmental modulation, and evolution. Annu Rev Plant Biol 56:99–131

Gleitz M, Kukert H, Riebesell U, Dieckmann GS (1996) Carbon acquisition and growth of Antarctic sea ice diatoms in closed bottle incubations. Mar Ecol Prog Ser 135:169–177

Goldman JAL, Kranz SA, Young JN, Tortell PD, Stanley RHR, Bender ML, Morel FM (2015) Gross and net production during the spring bloom along the Western Antarctic Peninsula. New Phytol 205:182–191

Hammes F, Vital M, Egli T (2010) Critical evaluation of the volumetric 'bottle effect' on microbial batch growth. Appl Environ Microbiol 76:1278–1281

Hopkinson B, Xu Y, Shi D, McGinn PJ, Morel FM (2010) The effect of CO_2 on the photosynthetic physiology of the phytoplankton in the Gulf of Alaska. Limnol Oceanogr 55:2011–2024

Hopkinson BM, Dupont CL, Allen AE, Morel FMM (2011) Efficiency of the CO_2-concentrating mechanism of diatoms. Proc Natl Acad Sci USA 108:3830–3837

Hopkinson BM, Meile C, Shen C (2013) Quantification of extracellular carbonic anhydrase activity in two marine diatoms and investigation of its role. Plant Physiol 162: 1142–1152

Keller K, Morel FMM (1999) A model of carbon isotopic fractionation and active carbon uptake in phytoplankton. Mar Ecol Prog Ser 182:295–298

Knap AH, Michaels A, Close AR, Ducklow H, Dickson AG (1996) Protocols for the Joint Global Ocean Flux Study (JGOFS) core measurements. JGOFS, Reprint of the IOC Manuals and Guides No 29, UNESCO 1994 19, Paris

Kranz SA, Young JN, Hopkinson B, Goldman JAL, Tortell PD, Morel FMM (2015) Low temperature reduces the energetic requirement for the CO_2 concentrating mechanism in diatoms. New Phytol 205:192–201

Le Quéré C, Rödenbeck C, Buitenhuis ET, Conway TJ and others (2007) Saturation of the Southern Ocean CO_2 sink due to recent climate change. Science 316:1735–1738

Losh JL, Morel FMM, Hopkinson BM (2012) Modest increase in the C:N ratio of N-limited phytoplankton in the California Current in response to high CO_2. Mar Ecol Prog Ser 468:31–42

Losh JL, Young JN, Morel FM (2013) Rubisco is a small fraction of total protein in marine phytoplankton. New Phytol 198:52–58

McMinn A, Müller MN, Martin A, Ryan KG (2014) The response of Antarctic sea ice algae to changes in pH and CO_2. PLoS ONE 9:e86984

Mehrbach C, Culberson CH, Hawley JE, Pytkowicz RM (1973) Measurement of the apparent dissociation constants of carbonic acid in seawater at atmospheric pressure. Limnol Oceanogr 18:897–907

Mitchell C, Beardall J (1996) Inorganic carbon uptake by an Antarctic sea-ice diatom, *Nitzschia frigida*. Polar Biol 16: 95–99

Montes-Hugo M, Doney SC, Ducklow HW, Fraser W, Martinson D, Stammerjohn SE, Schofield O (2009) Recent changes in phytoplankton communities associated with rapid regional climate change along the Western Antarctic Peninsula. Science 323:1470–1473

Nakajima K, Tanaka A, Matsuda Y (2013) SLC4 family transporters in a marine diatom directly pump bicarbonate from seawater. Proc Natl Acad Sci USA 110:1767–1772

Pinckney JL, Paerl HW, Harrington MB, Howe KE (1998) Annual cycles of phytoplankton community-structure and bloom dynamics in the Neuse River Estuary, North Carolina. Mar Biol 131:371–381

Raven JA, Johnston AM, Kubler JE, Korb R and others (2002) Seaweeds in cold seas: evolution and carbon acquisition. Ann Bot 90:525–536

Raven JA, Giordano M, Beardall J, Maberly SC (2011) Algal and aquatic plant carbon concentrating mechanisms in relation to environmental change. Photosynth Res 109: 281–296

Raven JA, Beardall J, Giordano M (2014) Energy costs of carbon dioxide concentrating mechanisms in aquatic organisms. Photosynth Res 121:111–124

Reinfelder JR (2011) Carbon concentrating mechanisms in eukaryotic marine phytoplankton. Annu Rev Mar Sci 3: 291–315

Riebesell U, Wolf-Gladrow DA, Smetacek V (1993) Carbon dioxide limitation of marine phytoplankton growth rates. Nature 361:249–251

Schulz KG, Bellerby RGJ, Brussaard CPD, Büdenbender J and others (2013) Temporal biomass dynamics of an Arctic plankton bloom in response to increasing levels of atmospheric carbon dioxide. Biogeosciences 10:161–180

Schumann A, Goss R, Jakob T, Wilhelm C (2007) Investigation of the quenching efficiency of diatoxanthin in cells of *Phaeodactylum tricornutum* (Bacillariophyceae) with different pool sizes of xanthophyll cycle pigments. Phycologia 46:113–117

Sharkey TD, Berry JA (1985) Carbon isotope fractionation in algae as influenced by an inducible CO_2 concentrating mechanism. In: Lucas W, Berry JA (eds) Inorganic carbon uptake by aquatic photosynthetic organisms. Am Soc Plant Physiol, Rockville, MD, p 389–401

Silverman DN (1982) Carbonic anhydrase: Oxygen-18 exchange catalyzed by an enzyme with rate-contributing proton-transfer steps. Methods Enzymol 87:732–752

Sobrino C, Ward ML, Neale PJ (2008) Acclimation to elevated carbon dioxide and ultraviolet radiation in the diatom *Thalassiosira pseudonana*: effects on growth, photosynthesis, and spectral sensitivity of photoinhibition. Limnol Oceanogr 53:494–505

Timmermans KR, Gerringa LJA, de Baar HJW, van der Wagt B, Veldhuis MJW, de Jong JTM, Croot P (2001) Growth rates of large and small Southern Ocean diatoms in relation to availability of iron in natural seawater. Limnol Oceanogr 46:260–266

Tortell PD, Rau GH, Morel FM (2000) Inorganic carbon acquisition in coastal Pacific phytoplankton communities. Limnol Oceanogr 45:1485–1500

Tortell PD, Payne CD, Guenguen C, Strzepek RF, Boyd PW, Rost B (2008a) Inorganic carbon uptake by Southern Ocean phytoplankton. Limnol Oceanogr 53:1266–1278

Tortell PD, Payne CD, Li Y, Trimborn S and others (2008b) CO_2 sensitivity of Southern Ocean phytoplankton. Geophys Res Lett 35:L04605, doi:10.1029/2007GL032583

Tortell PD, Trimborn S, Li Y, Rost B, Payne CD (2010) Inorganic carbon utilization by Ross Sea phytoplankton across natural and experimental CO_2 gradients. J Phycol 46:433–443

Tortell PD, Mills MM, Payne CD, Maldonado MT and others (2013) Inorganic C utilization and C isotope fractionation by pelagic and sea ice algal assemblages along the Antarctic continental shelf. Mar Ecol Prog Ser 483:47–66

Tortell PD, Asher EC, Ducklow HW, Goldman JAL and others (2014) Metabolic balance of coastal Antarctic waters revealed by autonomous pCO_2 and $\Delta O_2/Ar$ measurements. Geophys Res Lett 41:6803–6810

Trimborn S, Brenneis T, Sweet E, Rost B (2013) Sensitivity of Antarctic phytoplankton species to ocean acidification: growth, carbon acquisition, and species interaction. Limnol Oceanogr 58:997–1007

Venrick EL, Beers JR, Heinbokel JF (1977) Possible consequences of containing microplankton for physiological rate measurements. J Exp Mar Biol Ecol 26:55–76

Welschmeyer NA (1994) Fluorometric analysis of chlorophyll *a* in the presence of chlorophyll *b* and phaeopigments. Limnol Oceanogr 39:1985–1992

Whitney SM, Shaw DC, Yellowlees D (1995) Evidence that some dinoflagellates contain a ribulose-1,5-bisphosphate carboxylase/oxygenase related to that of the alphaproteobacteria. Proc Biol Sci 259:271–275

Woodger FJ, Badger MR, Price GD (2005) Regulation of cyanobacterial CO_2-concentrating mechanisms through transcriptional induction of high-affinity C_i-transport systems. Can J Bot 83:698–710

Young JN, Goldman JAL, Kranz SA, Tortell PD, Morel FMM (2015) Slow carboxylation of Rubisco constrains the rate of carbon fixation during Antarctic phytoplankton blooms. New Phytol 205:172–181

Zhang HN, Byrne RH (1996) Spectrophotometric pH measurements of surface seawater at *in-situ* conditions: absorbance and protonation behavior of thymol blue. Mar Chem 52:17–25

Zhang J, Quay PD, Wilbur DO (1995) Carbon-isotope fractionation during gas-water exchange and dissolution of CO_2. Geochim Cosmochim Acta 59:107–114

Editorial responsibility: Antonio Bode, A Coruña, Spain

Submitted: November 6, 2014; Accepted: May 6, 2015
Proofs received from author(s): July 10, 2015